

# Augmentation of GPS for Ship Navigation in Constricted Water Ways

S. Ryan, M. Petovello, and G. Lachapelle  
*Department of Geomatics Engineering*  
*The University of Calgary*

## BIOGRAPHIES

Sam Ryan holds a BEng (1992) from Memorial University, St. John's, Newfoundland and is an Electronic Systems Engineer in the Marine Technical and Support Services Directorate of the Canadian Coast Guard. At present he is on educational leave to obtain an MSc. in Geomatics Engineering at The University of Calgary.

Mark Petovello is a BSc. student in the Department of Geomatics Engineering, The University of Calgary. He expects to complete his degree in April 1998 and pursue a MSc. in Geomatics Engineering.

Dr. Gérard Lachapelle is Professor and Head of the Department of Geomatics Engineering where he is responsible for teaching and research related to positioning, navigation, and hydrography. He has been involved with GPS developments and applications since 1980.

## ABSTRACT

Vessels navigating in constricted water ways require reliable and accurate positions. In these water ways, the line-of-sight GPS signals are often masked by obstructions, resulting in degraded geometry and accuracy at best, and unavailability or unreliable positions at worst. The use of combined GPS-GLONASS results in a dramatic increase in the number of satellites available above the horizon. Simulation analysis was used to show the improvement achievable by augmenting DGPS with single point GLONASS, differential GLONASS, and height constraint. By running the simulation over a 24 hour period the complete GPS constellation was analyzed. To validate the results from the simulation, field trials were conducted under various GPS and GPS-GLONASS masking angles. Two Ashtech GG24™ receivers were used for these trials. For both the simulation and field trials the availability and reliability performance were analyzed as a function of signal obstruction elevation and the types of augmentation that were implemented. These results clearly demonstrate the advantage of augmenting

GPS with GLONASS and a height constraint, especially for ship navigation in constricted water ways.

## INTRODUCTION

Both the Canadian Coast Guard (CCG) and United States Coast Guard (USCG) are completing work on their public marine Differential GPS (DGPS) systems. Initial operational capability of the services were declared in August 1996 and January 1996 for the CCG and USCG respectively. The levels of service being provided by the two coast guards are essentially identical, and both systems use Ashtech reference stations (based on the Ashtech Z-12™ receiver). The horizontal accuracy specification for both systems is 10 m (95% of the time), however better accuracy can be achieved by using high end receivers. Table 1 lists some of the marine accuracy requirements.

*Table 1 Marine Accuracy Requirements*

Applications	2DRMS Accuracy
Safety of Navigation [FRP, 1996]	
Ocean Phase	1.8 - 3.7 km
Coastal Phase	460 m
Harbor and Harbor Approach	8 - 20 m
Inland Waterways	2 - 5 m
Other Desirable Requirements [Lachapelle, 1997]	
Placing Aids to Navigation	< 5 m
Resource Exploration	1 - 5 m
3D Navigation in constricted Channels	< 10 cm

Both marine DGPS systems should meet these accuracy requirements, except of course the 10 cm<sub>3D</sub> navigation requirement. The 10 cm<sub>3D</sub> accuracy level can only be met using an on-the-fly carrier phase system, which is outside the scope of the current marine DGPS systems and this

paper. Although the accuracy requirements of the systems can be achieved, questions remain as to the reliability of the DGPS corrections.

Unfortunately, hard numbers for the reliability of the marine DGPS corrections are not available, however the methodology used to ensure the corrections are reliable is sound and is presented below. The general configuration of the CCG and USCG DGPS sites are similar but not identical, and the following discussion only applies to the CCG sites [Ryan, 1997]. All of the equipment installed at a CCG site is completely redundant and includes:

- 1) Two reference stations (RS)
- 2) Two integrity monitors (IM)
- 3) Two control station computers
- 4) Two programmable logic controllers
- 5) Two phone lines and two modems
- 6) Dual radiobeacon transmitters

The hardware reliability of the DGPS broadcast exceeds 99.7%. This value is based on the equipment's mean time between failure and mean time to repair values. When the radiobeacon is removed from the reliability analysis the remaining GPS and control equipment's hardware reliability exceeds 99.9%. Therefore, due to the redundant configuration of the DGPS sites, the broadcast is extremely reliable from a classical black box replacement viewpoint.

However, this does not completely address the reliability of the actual corrections transmitted to the marine users. The installations of the DGPS sites were done to maximize the reliability of the corrections. The GPS antennas were situated to minimize multipath and maximize satellite visibility. To help reduce multipath the GPS antennas also contain either a ground plane or a choke ring. The goal is to have multipath-free observables for all satellites above the horizon. In real time the GPS corrections are checked on the following three levels:

- 1) RS checks the magnitude of each PRC and RRC
- 2) IM checks the magnitude of each PRR and RRR
- 3) IM checks the Horizontal Position Error

If the pseudorange corrections (PRC) or range rate corrections (RRC) exceed a predefined threshold the corrections are not broadcast to the user. The IM then checks the pseudorange residuals (PRR) and range rate residuals (RRR), if these exceed a predefined threshold the RS stops sending corrections for the offending satellite. Finally if the IM's position error is outside of tolerance, the marine users are immediately notified to stop using the corrections. With these integrity checks, the quality installation, and the redundant equipment, one can be assured that the corrections are reliable. However, the system cannot prevent problems from occurring at the user's end. Potential problems include the following:

- 1) User multipath

- 2) User receiver blunders (wrong code, incorrect time tags, etc)
- 3) Troposphere or ionosphere modeling problems
- 4) Masking effects resulting in a weak geometry

Although the broadcast DGPS corrections are reliable, this does not guarantee a reliable position for the user due to the above concerns. Evaluating the user's positioning reliability and various augmentations that will improve this reliability is the focus of this paper.

In order to evaluate the reliability of the marine user's position, DGPS was sequentially augmented with single point GLONASS (GLONASS), differential GLONASS (DGLONASS), and a height constraint. Thus the following six positioning methods were analyzed:

- 1) DGPS alone
- 2) DGPS and a height constraint
- 3) DGPS and GLONASS
- 4) DGPS, GLONASS, and a height constraint
- 5) DGPS and DGLONASS
- 6) DGPS, DGLONASS, and a height constraint

These methods were analyzed under four isotropic mask angles (5°, 10°, 15°, and 20°) to see if the improvement is mask angle dependent.

To evaluate the reliability differences between the six positioning methods, two analysis procedures were used. First a simulation analysis was conducted over a 24 hour period to determine how the augmentations improved the availability and reliability of the position solution. Second data collected using two Ashtech GG24™ integrated GPS-GLONASS receivers was analyzed to illustrate how the six positioning methods performed using actual data containing user generated blunders. Before the results from the simulation and the field test are presented, the reliability theory used for the analysis is presented in the next section.

## RELIABILITY THEORY

*Reliability refers to the controlability of observations, that is, the ability to detect blunders and to estimate the effects that undetected blunders may have on a solution. [Leick, 1995]*

Reliability can be sub-divided into internal and external reliability. Internal reliability quantifies the smallest blunder that can be detected through statistical testing of the residuals. This implies that the position solution is not unique, hence redundancy must exist in order to detect a blunder. Once the internal reliability has been determined, external reliability quantifies the impact that an undetected blunder can have on the unknown parameters.

The amount of redundancy ( $v_i$ ) that each observation adds to the solution is given by equation 1.

$$v_i = (C_{\hat{r}}C_1^{-1})_{ii} \quad \text{Eq. \#1}$$

where  $C_{\hat{r}}$  is the covariance matrix of the residuals

$C_1$  is the covariance matrix of the observations

By investigating the residual covariance matrix in equation 2, it is evident that individual redundancy numbers for each observation must range from 0 to 1.

$$C_{\hat{r}} = C_1 - A(A^T C_1^{-1} A)^{-1} A^T \quad \text{Eq. \#2}$$

where  $A$  is the design matrix

In order to detect a blunder in an observation, a statistical test must be done on the residuals. The underlying assumption is that the residuals are normally distributed and that a blunder, while biasing the residual, does not change its variance. There are two types of errors that can be made when performing any statistical test. A Type I error occurs whenever a good observation is rejected. The probability associated with a Type I error is denoted  $\alpha$ . A Type II error occurs whenever a bad observation is accepted. The probability associated with a Type II error is denoted  $\beta$ . Figure 1 shows a graphical representation of the relationship between the Type I/II errors and the bias in the standardized residual called the non centrality parameter  $\delta_o$ . By selecting values for  $\alpha$  and  $\beta$ ,  $\delta_o$  can be determined, as shown in Table 2.

Table 2 Non Centrality Parameter [Leick, 1995]

$\alpha$	$\beta$	$\delta_o$
5.0%	20%	2.80
2.5%	20%	3.10
5.0%	10%	3.24
2.5%	10%	3.52
0.1%	20%	4.12
0.1%	10%	4.57

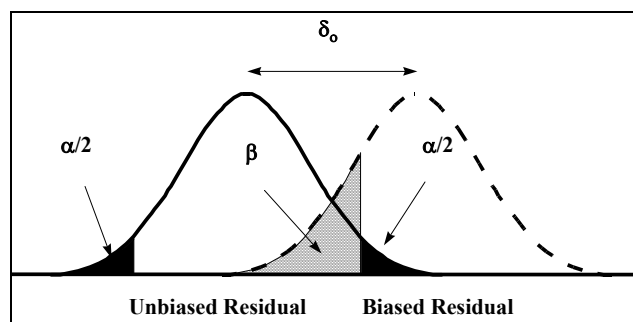


Figure 1 Type I/II Errors and Non Centrality Parameter

Once  $\delta_o$  is generated, the smallest blunder that can be detected through statistical testing is given by equation 3, and is termed the Marginally Detectable Blunder (MDB).

4. Data:

a) Date of Ephemeris: November 17-18, 1997

$$\text{MDB}_i \Rightarrow |\nabla_i| = \frac{\delta_o \sigma_{l_i}}{\sqrt{v_i}} \quad \text{Eq. \#3}$$

Each observation has a different MDB since the redundancy number for each observation is different. Therefore, it is desirable for all of the observations' redundancy numbers to be approximately equal and close to unity, since the position is only as robust as its lowest redundancy number. If this is the case the solution does not have any weaknesses due to blunders.

Once the MDB's for each observation have been calculated, the impact of each blunder on the unknown parameters must be determined. The underlying assumption is that only one blunder can occur any one time. Therefore, each MDB is applied separately to assess its impact on the parameters via equation 4.

$$\Delta X_i = -C_x A^T C_1^{-1} \nabla_o \quad \text{Eq. \#4}$$

where  $\nabla_o$  is a column vector containing all zero's except for the MDB in the  $i^{\text{th}}$  position. Equation 4 reflects the external reliability of the solution. Since horizontal positioning is paramount in marine applications the horizontal error corresponding to each MDB is calculated using equation 5.

$$\text{Horizontal Error}_i = \sqrt{\Delta \phi_i^2 + \Delta \lambda_i^2} \quad \text{Eq. \#5}$$

The largest horizontal error is termed the Maximum Horizontal Error (MHE) and represents the external reliability in marine positioning applications.

## SIMULATION DESCRIPTION

In order to determine the theoretical improvement in availability and reliability by augmenting DGPS with GLONASS and a height constraint, numerous simulations were conducted. The following parameters define the simulation parameters used:

- Positioning Methods:
  - DGPS alone
  - DGPS and a height constraint
  - DGPS and GLONASS
  - DGPS, GLONASS, and a height constraint
  - DGPS and DGLONASS
  - DGPS, DGLONASS, and a height constraint
- Reliability Parameters:
  - $\alpha = 0.1\%$ ,  $\beta = 10\%$ , and  $\delta_o = 4.57$
- Isotropic Mask Angles :
  - 5°
  - 10°
  - 15°
  - 20°

b) Duration: 24 hours

c) Location: 50° N 114° W

- d) 25 GPS satellites available
- e) 15 GLONASS satellites available

For the simulation analysis conservative values for the observation variances were used;

- 1) DGPS = 9 m<sup>2</sup>
- 2) GLONASS = 64 m<sup>2</sup>
- 3) DGLONASS = 9 m<sup>2</sup>
- 4) height constraint = 9 m<sup>2</sup>.

Although these variances may seem high, the desire was to simulate a marine quality receiver [Hall, 1997 and Bazarov, 1996].

The reliability algorithm used for the simulations was conservative since it assumed the residual testing is done epoch by epoch using no apriori knowledge of the trajectory.

The improvement by augmenting DGPS with GLONASS and a height constraint were evaluated by looking at the improvement in availability (HDOP for the marine case) and reliability (MHE). When the variances of the observations are equal the HDOP is based solely on geometry. However in the case where GLONASS (single point) is used to augment DGPS, there is a large difference between the two variances, and a weighted HDOP must be calculated as shown in equation 6. Since DGPS is the basic system all other variances are compared with it.

$$DOP = \sqrt{\text{trace}([A^T P A]^{-1})}$$

$$HDOP = \sqrt{NDOP^2 + EDOP^2} \quad \text{Eq. \#6}$$

$$P = \begin{bmatrix} \frac{\sigma_{DGPS}^2}{\sigma_{DGPS}^2} = 1 & 0 & 0 \\ 0 & \frac{\sigma_{DGPS}^2}{\sigma_{GLONASS}^2} = \frac{9}{64} & 0 \\ 0 & 0 & \frac{\sigma_{DGPS}^2}{\sigma_{Height}^2} = 1 \end{bmatrix}$$

The weight matrix (P) is identity whenever DGPS is augmented with DGLONASS and/or a height constraint, since for such a simulation they all share the same variance. Only when GLONASS (single point) is used is the weight matrix (P) not identity. In this case the diagonal values for the rows corresponding to GLONASS satellites are 9/64 while all of the other entries on the diagonal are unity. In the simulation the height constraint is added as a quasi-observable to the design matrix (A) and therefore it is also included in the weight matrix (P).

### SIMULATION RESULTS

The results from the simulations have been summarized in Figure 2 and Figure 3 for the HDOP and MHE respectively. The results for the four mask angles and the

six positioning methods have all been included on the same graph. For each case, the 95 and 99 percentiles were calculated using a one minute data sampling interval over 24 hours. The two percentiles were plotted for each method and each mask angle.

The HDOP improvement by augmenting DGPS can be seen graphically as the magnitude of the slope of the 95 or 99 percentile lines. As the mask angle increases the slope of the 95 percentile curve also increases, thus the percentage improvement through augmentation also increases. In the 5° mask angle case the 95% HDOP varies from 1.2 (DGPS) to 0.9 (DGPS + DGLONASS + Height). The HDOP is improved through augmentation but the improvement is not impressive. For the 20° mask angle case the 95% HDOP improves from 2.9 (DGPS) to 1.6 (DGPS + DGLONASS + Height). Although there is a larger improvement in the HDOP at the higher masking angles, this type of performance improvement would not, by itself, justify augmenting DGPS with DGLONASS.

The results obtained by augmenting DGPS with GLONASS (single point) fall directly between the DGPS and DGPS with DGLONASS values. This is expected since whenever additional observations are added to an adjustment the HDOP must be improved, and the magnitude of the improvement will be a function of the relative variances of the observations.

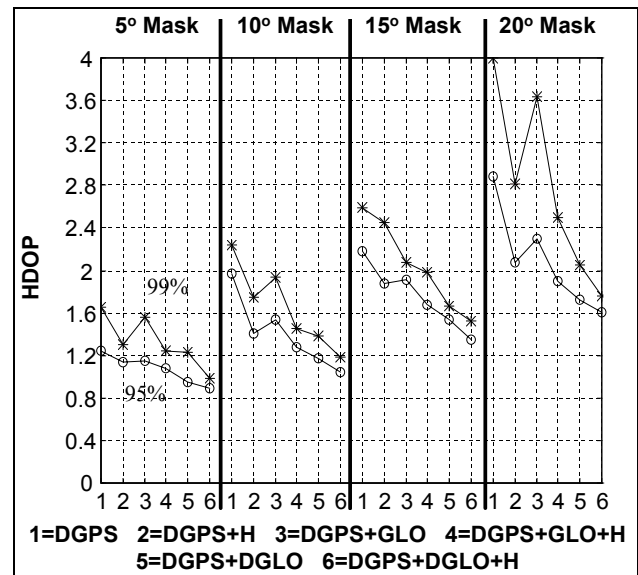


Figure 2 HDOP - 4 Mask Angles - 6 Methods

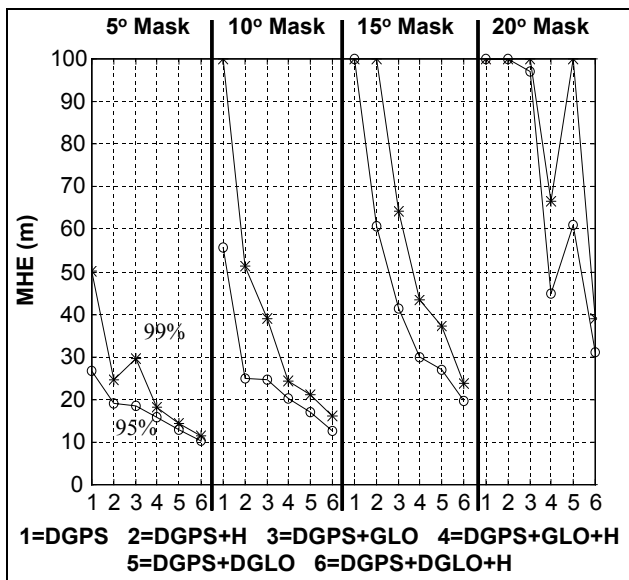


Figure 3 MHE - 4 Mask Angles - 6 Methods

The reliability (MHE) improvement obtained by augmenting DGPS, as shown in Figure 3, is much more dramatic than for the HDOP. Even for the 5° mask angle case the 95% MHE improves from 27 m to 10 m. This is almost a 3 to 1 improvement. As the mask angle increases the improvement is even more pronounced. The 95%

MHE for the 15° mask angle case ranges from > 100 m to 20 m, a 5 to 1 improvement.

Even if only GLONASS (single point) is used to augment DGPS there is still a dramatic reliability improvement especially for higher mask angles. For the 15° mask angle case the reliability is improved from > 100 m to 41 m by adding GLONASS, a 2.5 to 1 improvement. Further improvements are obtained by introducing a height constraint as depicted in Figure 3. This demonstrates that reliability is the big winner when DGPS is augmented with GLONASS/DGLONASS and height.

Figure 4 and Figure 5 plot the HDOP and MHE for the six positioning methods versus time, using a 15° mask angle, respectively. Figure 4 shows that as DGPS is augmented with GLONASS, DGLONASS and height, the HDOP spikes are gradually reduced and the overall HDOP level is decreased. The maximum HDOP for the DGPS case is 3.0. While this is a large HDOP value it would not preclude marine navigation. Therefore, the addition of GLONASS and a height constraint do not seem to significantly improve the navigation performance.

While the HDOP curves in Figure 4 show that it is acceptable to navigate with DGPS alone, the MHE versus time curves shown in Figure 5 show that DGPS alone

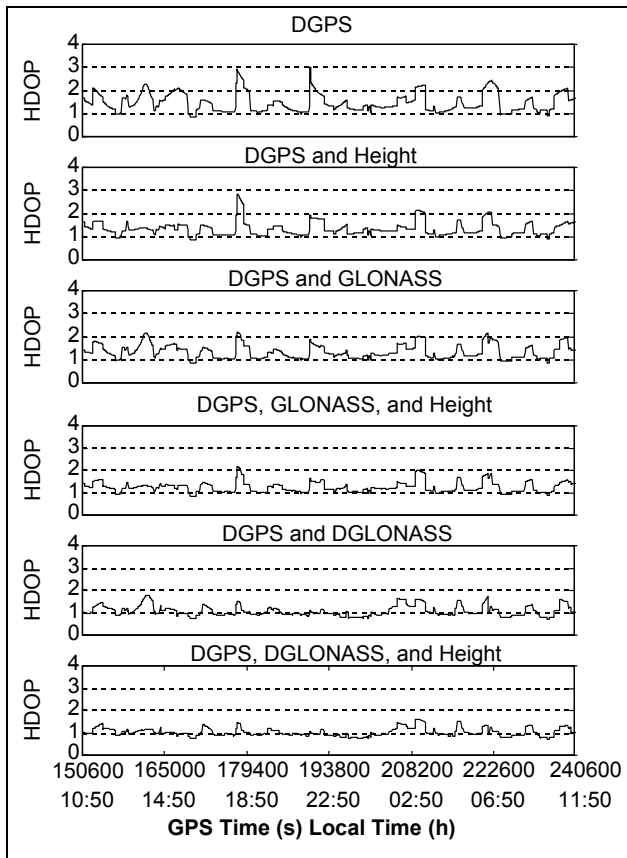


Figure 4 HDOP vs Time - 15° Mask Angle - 6 Methods

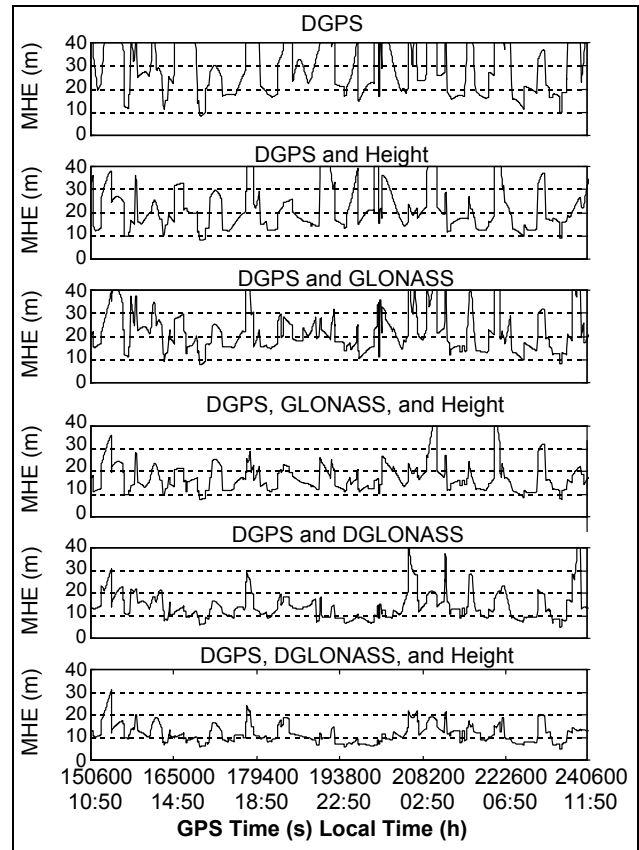


Figure 5 MHE vs Time - 15° Mask Angle - 6 Methods

does not provide reliable navigation opportunities. The DGPS 95% MHE is > 100 m in this case, and there are numerous spikes that are > 40 m. However, as augmentations are added to DGPS there is a gradual lowering and smoothing in the MHE curves. In the most augmented case (DGPS+DGLONASS+Height) almost all of the MHE's are below 20 m.

In addition to running the simulations for the 50° N latitude, two additional latitudes were also simulated, specifically 25° N and 75° N. The 25° N simulation could be applied to the Gulf of Mexico, the 50° N simulation is representative of the St. Lawrence Seaway, and 75° N is representative of the Canadian Arctic. All of the above simulations were run for these additional two latitudes and similar trends were observed in the results. Thus,

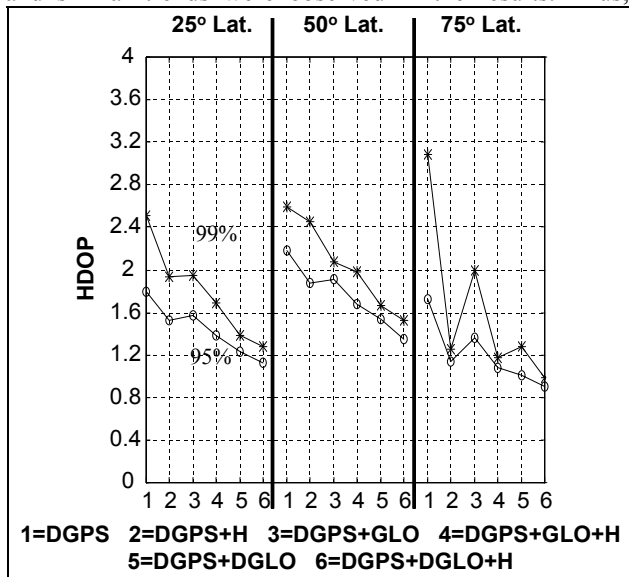


Figure 6 HDOP - 15° Mask Angle - 3 Latitudes

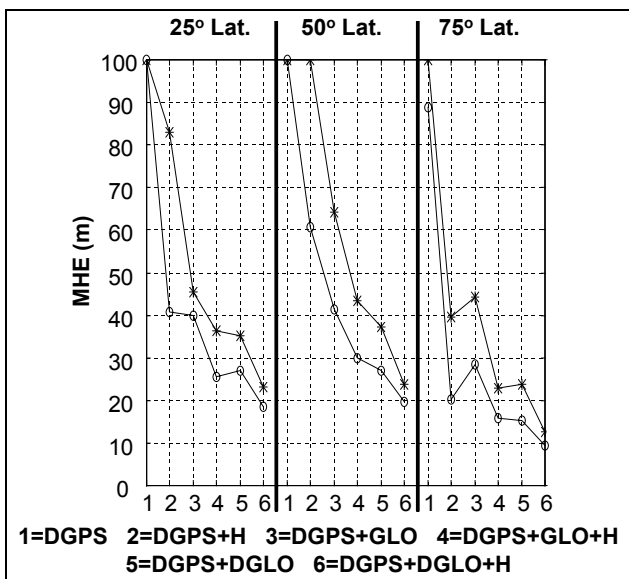


Figure 7 MHE - 15° Mask Angle - 3 Latitudes

instead of showing all of the graphs for the additional two latitudes, Figure 6 and Figure 7 show the HDOP and MHE results respectively, for the three latitudes using a 15° mask angle. Due to the different satellite geometries at the three latitudes the HDOP and MHE curves are not identical, however the same general trends are present. Regardless of the latitude, the magnitude of the improvement in MHE is much greater than that of the HDOP.

The selection of the single point GLONASS variance affects both the HDOP and MHE analyses. To test these affects, DGPS was augmented with GLONASS (single point) using different variances for the GLONASS observable. Figure 8 and Figure 9 show the HDOP and MHE results respectively when six different GLONASS variances are used. The corresponding standard deviations ( $\sigma_{glo}$ ) are shown on the x-axis for each isotropic mask angle. Note that  $\sigma_{glo} = 3$  m corresponds to the DGLONASS variance above and  $\sigma_{glo} = 8$  m corresponds to the GLONASS (single point) variance. The other values were plotted to show the sensitivity of the results to changes in the single point GLONASS variance.

Figure 8 shows that the slope of the percentile lines gradually increases as the mask angle is increased. However, even at 20° the 95% HDOP curve only shows a small difference between  $\sigma_{glo} = 3$  m and  $\sigma_{glo} = 14$  m, 1.7 to 2.5. Thus in general, HDOP is not sensitive to changes in the GLONASS variance for these mask angles.

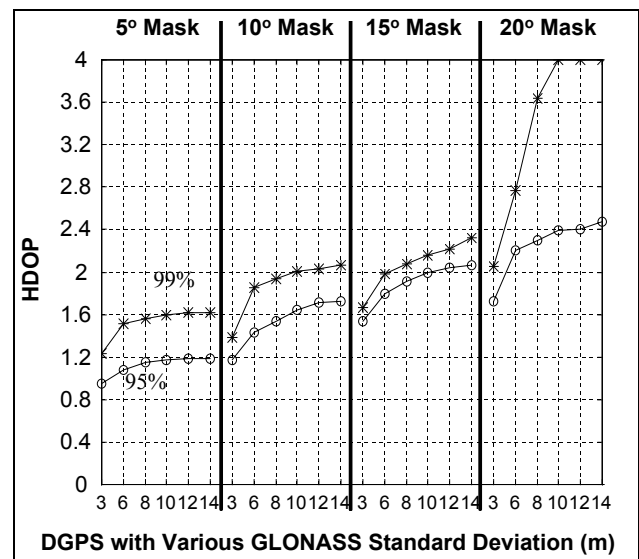


Figure 8 HDOP - 4 Mask Angles - 6 GLONASS Variance

As expected, the sensitivity of the results for the MHE is much more pronounced than for HDOP. This is shown in Figure 9. The slopes of all the lines increase dramatically as the mask angle is increased. Take for example the 95% MHE curve for the 15° mask angle case, the MHE varies from 27 m ( $\sigma_{glo} = 3$  m) to 58 m ( $\sigma_{glo} = 14$  m). The difference

between the MHE's is significant and illustrates the importance of having accurate GLONASS observables.

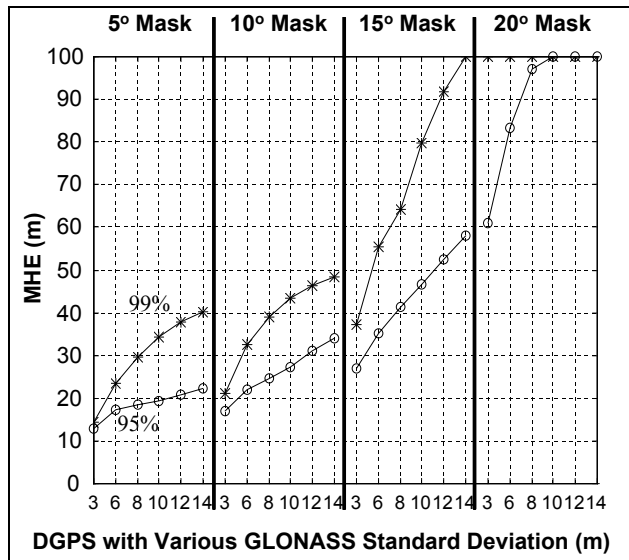


Figure 9 MHE - 4 Mask Angles - 6 GLONASS Variance

### ASHTECH GG24™ FIELD TEST

While the GPS and GLONASS almanacs and ephemerides were being collected for the simulation analysis, the GPS and GLONASS raw observables were also collected using the Ashtech GG24™ integrated GPS-GLONASS receivers. Two GG24™ receivers were installed on the roof of the engineering building at the University of Calgary, one acting as the reference station and one as the remote station. One hour of raw measurements were collected and were processed using the University of Calgary's C<sup>3</sup>NAV<sup>2</sup>™ software package. The purpose of the field test was to confirm the simulation conclusions that augmenting DGPS greatly improves the reliability of the solution.

A ramping error was superimposed on each GPS satellite, (PRN # 1, 5, 7, 14, 15, 21, 25, 29, and 30), however processing was performed using only one biased satellite at a time. Figure 10 shows the error introduced on each satellite. In total four ramps were introduced on each GPS satellite during the one hour data set. The error was ramped at 0.5 m/s until it reached a maximum error or 50 m, held at 50 m for 100 s and then ramped back down to zero at -0.5 m/s. Therefore, each blunder lasted 300 s, and in total there were 1200 s of biased measurements introduced to each satellite. The six positioning methods that were used for the simulation and the same four isotropic mask angles were processed using C<sup>3</sup>NAV<sup>2</sup>™ to evaluate the reliability improvement. Since marine navigation was the concern, the horizontal position error (HPE) was calculated for each epoch. Epoch to epoch reliability analysis was performed to detect the blunder on the offending GPS satellite.

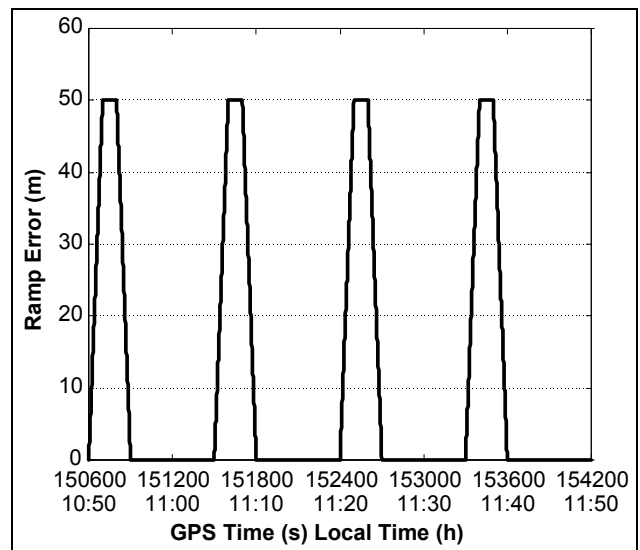


Figure 10 Blunder Introduced to each GPS Satellite

Figure 11 shows the HPE that occurred when the reliability checking was disabled using a 15° mask angle and the blunder was applied to PRN #1. Although the magnitude of the blunder was the same for the four ramps, the HPE is different for each ramp due to the changing geometry. As expected, when DGPS is

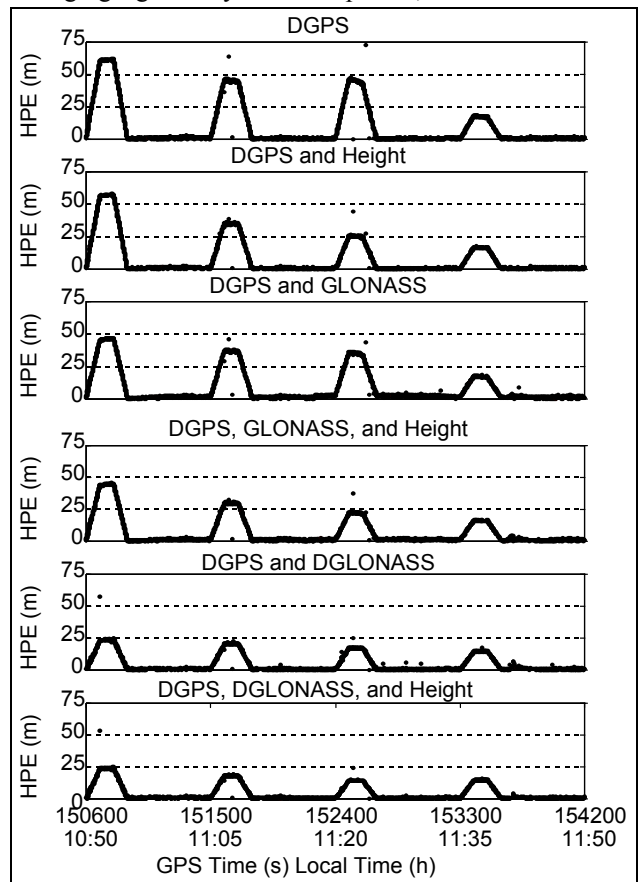


Figure 11 HPE - 15° Mask Angle - Ramp on PRN #1 Reliability Disabled



augmented the magnitude of the HPE is decreased. Even in the most constrained case (DGPS + DGLONASS + Height) the maximum HPE exceeded 25 m. Although one would normally expect reliability checking to be enabled, many commercial marine DGPS receivers do not use any reliability checking. Without reliability checking a blunder can play havoc with marine positioning.

Figure 12 shows the results when the same data is analyzed with reliability checking enabled. DGPS alone has difficulty detecting the first ramp, but the subsequent ramps are correctly detected. When single point GLONASS was added it greatly improved the performance during the first ramp however the beginning and end of the ramps still remained. Once DGLONASS was added the ramping errors are caught almost immediately, and the impact on the horizontal position is negligible. For all of the methods, the performance in the latter three ramps is much better, which is consistent with the previous figure.

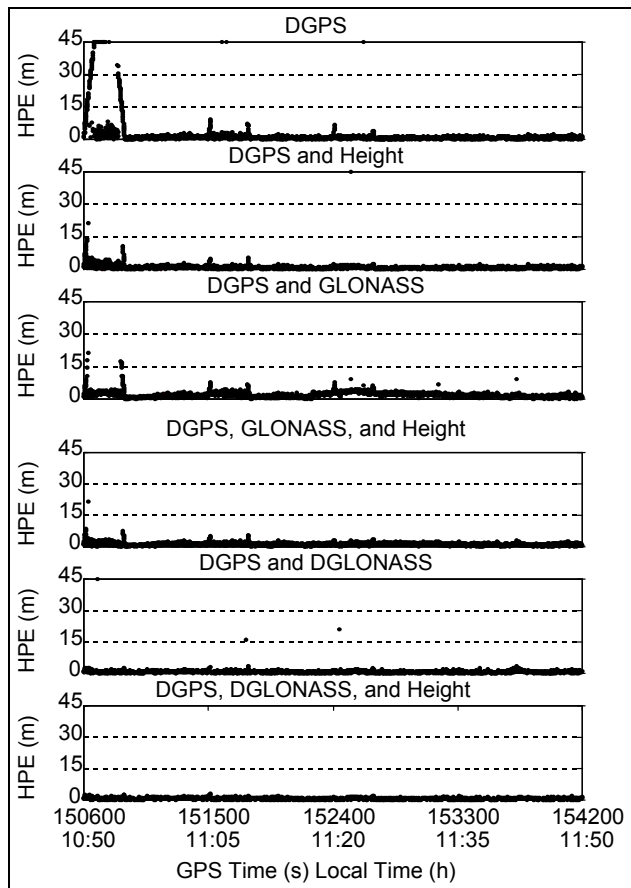


Figure 12 HPE - 15° Mask Angle - Ramp on PRN #1 Reliability Enabled

Figure 13 shows a close up of the first ramp to help emphasize the fault detection capabilities of the six positioning methods. Three things are evident from these graphs. First as DGPS is augmented the time taken to detected the error is shortened. Second, even before the

error is detected, the magnitude of the HPE is reduced. Finally, since an epoch by epoch reliability algorithm was implemented there are several spikes in the HPE indicating that the biased satellite could not be detected. Once DGLONASS is added the ramp is not noticeable on this scale thus indicating very reliability positions.

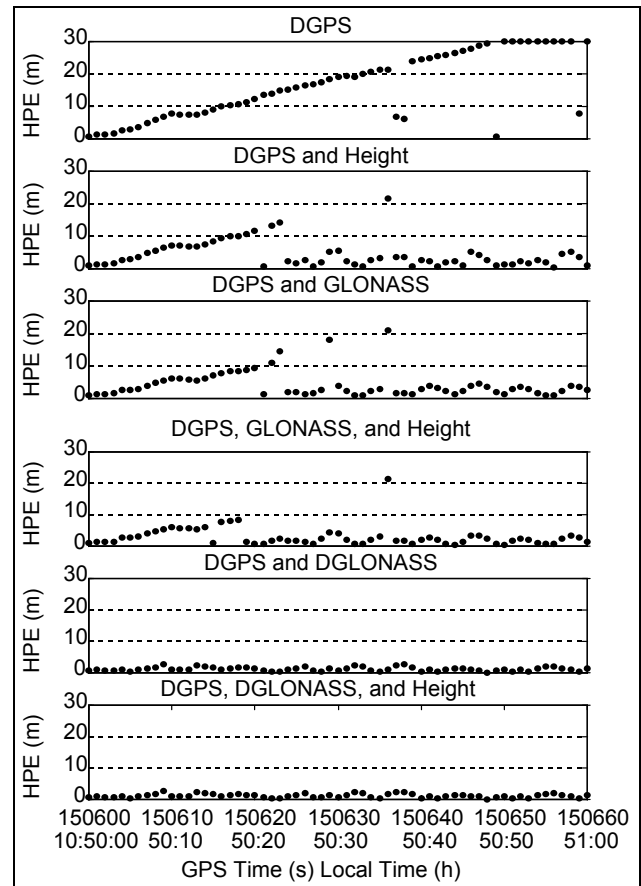


Figure 13 HPE - 15° Mask Angle - Ramp on PRN #1 Reliability Enabled - First Ramp

The previous results only reflect the ramp error on PRN #1 and a 15° mask angle. In total, ramps on nine GPS satellites, for four mask angles, were analyzed. Instead of showing these results individually, Figure 14 summarizes the results. Since the point of this analysis was to look at the reliability improvement, only the first ramp was analyzed. The results from the nine satellites were grouped together, thus in total 2700 data points were used. This was done for the six positioning methods over the four mask angles and the 95 and 99 percentiles were calculated and plotted. This is the same format that was used for the simulations. In this case actual GG24™ data was used for the analysis, thus the results will not match the simulation results but the trends should be the same. This is the indeed the case. At the lower mask angles of 5° and 10° the improvement in HPE is not dramatic. Augmenting DGPS improves the reliability of the positions, but not significantly. For instance the 95% HPE varies from 2.2 m to 1.4 m from the least to the most



augmented case using a 10° mask angle. However, at the 15° mask angle the results are more significant. The DGPS 95% HPE is > 10 m while the DGPS with DGLONASS is 1.5 m. This follows the same trends that were seen in the simulation results, that is, the real benefit of the augmentations occur during high masking conditions. While the reliability is improved during the lower mask cases it is not as dramatic as with the high mask angles.

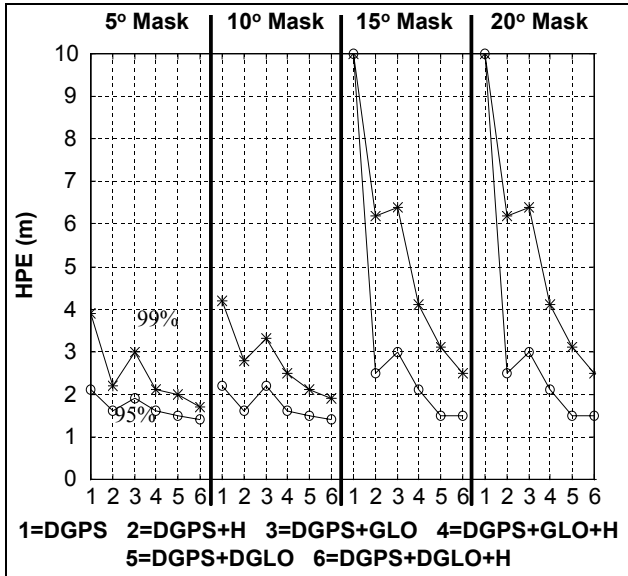


Figure 14 HPE - 4 Mask Angles - 6 Methods  
Reliability Enabled

## CONCLUSIONS

Even with the GLONASS constellation of only fifteen satellites that was used for the analysis, augmentation of DGPS with GLONASS and DGLONASS greatly improves both the reliability and the availability of the navigation system. The trends that were evident during the simulations and the actual field trials match each other. In all cases, augmenting DGPS with a height constraint and GLONASS improves both the HDOP and Horizontal Error. However, the true benefit of the augmentations occur during high mask angles.

Assuming that the GLONASS constellation is maintained, the benefits of integrating DGPS with GLONASS are very significant. During the short term, the public marine DGPS systems will only be broadcasting GPS corrections. However, as was shown by both the simulations and the field trials, augmentation of DGPS with even single point GLONASS improves the reliability. The optimum solution is obviously to use DGPS and DGLONASS together. Similarly a height constraint also improves the reliability of the positions and since the height is usually well known in marine applications this constraint should be implemented.

The reliability algorithm that was used for this analysis was fairly conservative. It was an epoch by epoch reliability analysis. This could be improved greatly by implementing a Kalman filter to improve the blunder detection and exclusion algorithm.

## REFERENCES

- 1996 *Federal Radionavigation Plan (FRP)*, U.S. Department of Transportation and U.S. Department of Defense. Report Number DOD-4650.5/DOT-VNTSC-RSPA-92-2.
- Bazarov, Y., 1996. *Introduction to Global Navigation Satellite System*. AGARD Lecture Series 207, June, 1996.
- Hall, T., B. Burke, M. Pratt, and P. Misra, 1997. *Comparison of GPS and GPS + GLONASS Positioning Performance*. Proceedings of ION-GPS-97, Institute of Navigation, 1997.
- Lachapelle, G., 1997. *Hydrography*. Department of Geomatics Engineering, University of Calgary Lecture Notes #10010. January, 1997.
- Leick, A., 1995, *GPS Satellite Surveying*, 2<sup>nd</sup> Edition. John Wiley & Sons, Inc. 1995.
- Ryan S., F. Forbes, and S. Wee, 1997. *Avoiding the Rocks - The Canadian Coast Guard Differential GPS System*. Proceedings of KIS97, Department of Geomatics Engineering, The University of Calgary, Banff (June), 1997.